HEFAT2012
9th International Conference on Heat Transfer, Fluid Mechanics and Thermodynamics
16 – 18 July 2012
Malta

NON-PERIODIC LIQUID MOVEMENT INSIDE THE GLASS NOZZLE DURING AIR BUBBLES DEPARTURES IN WATER

P. Dzienis, R. Mosdorf*, T. Wyszkowski
*Author for correspondence
Department of Mechanics and Applied Computer Science,
Białystok University of Technology,
ul. Wiejska 45C, 15-351 Białystok,
Poland,
E-mail: r.mosdorf@pb.edu.pl

ABSTRACT

In the paper the dynamics of liquid movement inside the glass nozzle submerged in the glass tank filled by distilled water has been analyzed. Considered liquid movement accompanied the process of bubble departures from the nozzle. There has been investigated the influence of air volume flow rate on the dynamics of liquid movement. The position of liquid-air interface inside the glass nozzle has been measured using the high speed camera. Recorded videos have been analyzed using the special software allowing to obtain the time series of position of air-liquid interface inside the glass nozzle. The dynamics of such obtained time series has been analyzed using the non-linear methods. The attractor reconstruction, correlation dimension and reoccurrence plot have been applied.

INTRODUCTION

The knowledge of bubble dynamics is of key importance in physical, biological and medical processes, and particularly in industrial applications. There are numerous physical parameters such as: physical properties of the two phases, gas flow rate, gas pressure, height of the liquid and gravity conditions which influence on the bubbles formation. The study of bubble dynamics is crucial to understand bubble-liquid and bubble-bubble interactions. Liquid penetration into capillaries during the bubble departures decides about the length of waiting time for appearing the next bubble. This process has been discussed in the papers [1, 2, 3]. In the present paper the dynamics of liquid movement inside the glass nozzle submerged in the glass tank filled by distillate water has been analyzed. Considered liquid movement accompanied the process of bubble departures from the nozzle. There has been investigated the influence of air volume flow rate on the dynamics of liquid movement. In the experiment bubbles were generated in tank (300x150x700), from glass nozzle with inner diameter equal to 1 mm. The experimental setup has been shown in Fig.1.

NOMENCLATURE

C	-	autocorrelation function, correlation function
D	-	dimension
DET	[%]	determinism
DIV	[1/samples]	divergence
f	[Hz]	frequency
L	[samples]	length of the diagonal line
$LAVG$	[samples]	average length of the diagonal lines
m	-	embedding dimension
N	-	number of samples
P	-	probability distribution
q	[l/min]	air volume flow rate
R	-	recurrence plot
RR	[%]	recurrence rate
t	[s]	time
TT	[samples]	trapping time
V	[samples]	length of the vertical line
w	[samples]	window wide
x	[pixels]	sample value

Special characters

θ	-	Heaviside function
ε	-	threshold distance
τ	[samples]	time delay

Subscripts

i,j	samole number
l	diagonal
v	vertical
2	correlation
max	maximum value
min	minimum value

The nozzle was placed on the bottom of the tank. The tank was filled with distillate water, with temperature about 20°C. The temperature was constant during the experiment. The air pressure fluctuations have been measured using the silicon pressure sensor MPX12DP. The air volume flow rate was measured using the flow meter and was changed from 0.0045 l/min to 0.125 l/min. The pressure was recorded using

the data acquisition system DT9800 series USB Function Modules for Data Acquisition Systems with sampling frequency of 2 kHz.

The bubble departure and liquid movement inside the nozzle were recorded with the high – speed camera – CASIO EX FX 1. The duration of each video was 20s. The recorded frames (600 fps) in grey scale, has been divided into frames (Fig.2.).

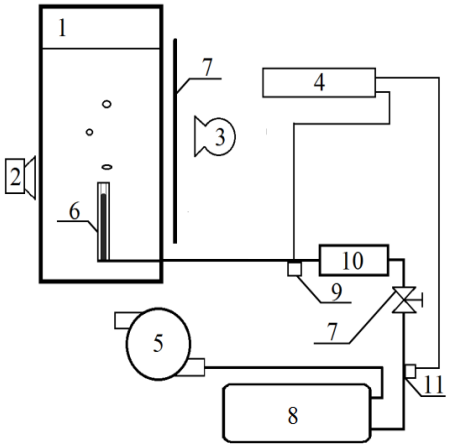

Figure 1 Experimental setup: 1 – glass tank, 2 - camera, 3 - light source,4 - computer acquisition system, 5 – air pump, 6 – glass nozzle, 7 - air valve, 8 - air tank, 9, 11 - pressure sensor, 10 - flow meter.

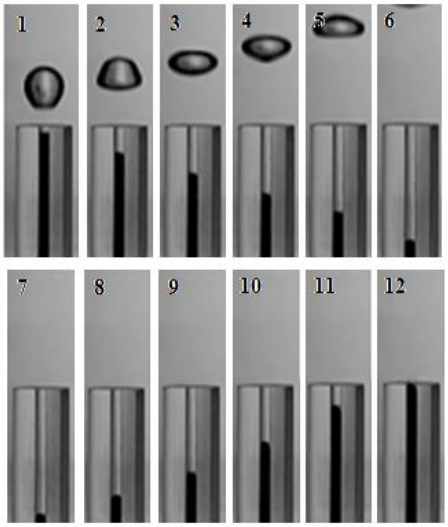

Figure 2 Liquid penetration into capillaries and the bubble departure

The depth of the liquid penetration was measured by a special program, which counted the number of lighter pixels in the frames. Then, the time series of depth of the liquid penetration has been received. For the selected gas flow, the length of the time series of depth of the liquid penetration was about 12 000 samples. The examples of recorded time series have been shown in Fig.3.

The frequency of bubble departures has been estimated using the FFT method. The mean frequency of bubble departures was changed in the range between 2 and 16 Hz. The dynamics of such obtained time series has been analyzed using non-linear methods. The attractor reconstruction, correlation dimension and recurrence plot have been applied for identification of properties of dynamics of liquid movement.

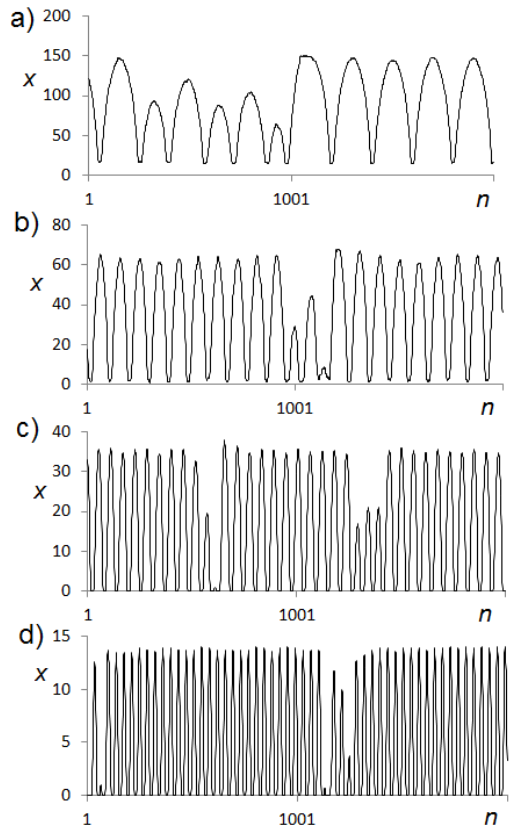

Figure 3 Time series of changing the position of air-liquid interface inside the glass nozzle for different air volume flow rates a) q = 0.00519 l/min, f = 2.56 Hz. b) q = 0.0132 l/min, f = 6.59 Hz. c) q = 0.0216 l/min, f = 10.62 Hz. d) q = 0.0334 l/min, f = 16.14 Hz.

NONLINEAR DATA ANALYSIS

The trajectories of nonlinear dynamical system in the phase space form objects called strange attractors of the structure resembling the fractal [7, 8]. The analysis of strange attractor gives us information about the properties of dynamical system such as system complexity and its stability. In nonlinear analysis the reconstruction of attractor in certain embedding dimension has been carried out using the stroboscope coordination. In this method subsequent co-ordinates of attractor points have been calculated basing on the subsequent samples, between which the distance is equal to time delay τ. The time delay is a multiplication of time between the samples. The nonlinear analysis of the experimental data is initiated by determining the time delay τ. For that purpose, the autocorrelation function is usually calculated. This function allows us to identify the correlation between subsequent samples. In case of chaotic data the value of autocorrelation

function rapidly decreases when τ increases. The value of the time delay τ is determined from the condition $C(\tau) \approx 0.5 * C(0)$ [7].

The correlation dimension D_2 is one of the characteristics of attractors, which allows us to identify the structure of attractors. It is defined by the following expression [7]:

$$D_2 = \lim_{d \to 0} \frac{1}{\ln(d)} ln C^2(d) \tag{1}$$

where: $C^2(d) = \frac{1}{N} \sum_i \left[\frac{1}{N} \sum_j \theta\left(d - |x_i - x_j|\right) \right]$

θ - Heaviside's step function that determines the number of attractor's point pairs of the distance shorter than d.

The correlation dimension allows us to estimate the number of independent variables describing the system. This number is estimated as the lowest integer number greater than the correlation dimension.

The recurrence plot (RP) visualizes the recurrence of states x_i in a phase space. The RP enables us to investigate the recurrence of a state in m-dimensional phase. The recurrence of a state at time i at a different time j is marked within black dots in the plot, where both axes are time axes. From the formal point of view the RP can be expressed as [9]:

$$R_{i,j} = \theta\left(\varepsilon - \left\| x_i - x_j \right\|\right),\ x_i \in \Re^m,\ i, j - 1 \ldots N \tag{2}$$

where N is the number of considered states x_i in m dimensional space, ε_i is a threshold distance, $\| \cdot \|$ a norm and $\Theta(\cdot)$ the Heaviside function.

Single, isolated recurrence points can occur if states are rare. Oscillating systems have RPs with diagonal oriented, periodic recurrent structures. For quasi-periodic systems, the distances between the diagonal lines are different. A diagonal line occurs when a segment of the trajectory runs parallel to another segment and the distance between trajectories is less than ε. The length of this diagonal line is determined by the duration of this phenomenon. Large changes in the dynamics cause appearance of white areas or bands in the RP. A vertical (horizontal) line indicates the time in which a state does not change or changes very slowly.

Coefficient *RR* (recurrence rate) is the percentage of recurrence points in the RP and is calculated as follows [9]:

$$RR = \frac{1}{N^2} \sum_{i,j=0}^{N} R_{i,j} \tag{3}$$

Coefficient *DET* (determinism) is the percentage of recurrence points which form diagonal lines greater than l_{min} [9]:

$$DET = \frac{\sum_{l=l_{min}}^{N} lP(l)}{\sum_{i,j}^{N} R_{i,j}} \tag{4}$$

where *P(l)* is the histogram of the lengths l of the diagonal lines.

Coefficient *LAVG* is the average length of diagonal lines and is calculated as follows [9]:

$$LAVG = \frac{\sum_{l=l_{min}}^{N} lP(l)}{\sum_{l=l_{min}}^{N} P(l)} \tag{5}$$

Coefficient L_{max} is the length of the longest diagonal line. Coefficient *DIV* (divergence) is the inverse of L_{max} [9]:

$$DIV = \frac{1}{L_{max}} \tag{6}$$

The value of coefficient *DIV* is related with the sum of the positive Lyapunov exponents [9].

Coefficient *TT* (trapping time) is the average length of the vertical lines greater than v_{min} [9]:

$$TT = \frac{\sum_{v=v_{min}}^{N} vP(v)}{\sum_{v=v_{min}}^{N} P(v)} \tag{7}$$

Coefficient V_{max} is the length of the longest vertical line

In the present analysis the recurrence plots were constructed for subsequent parts of analyzed time series. The subsequent parts of time series are selected from original time series by moving window with constant wide. Such parameters as correlation dimension and time delay have been calculated for the entire time series. The subsequent RPs have been constructed for the attractor reconstructed in embedding demission greater than correlation dimension. In this case the embedding dimension is the lowest integer number greater than attractor correlation dimension. For each window the above quantities characterizing the RP are determined. Finally, these quantities become the function of window location in time series. These functions describe the changes in time of dynamics of investigated system.

The following 6 functions have been considered: $RR(t, w, m, \tau, \varepsilon)$, $L(t, w, m, \tau, \varepsilon)$, $DET(t, w, m, \tau, \varepsilon)$, $DIV(t, w, m, \tau, \varepsilon)$, $TT(t, w, m, \tau, \varepsilon)$, $V_{max}(t, w, m, \tau, \varepsilon)$,

where t – time calculated as the multiplication of location of centre of window by time period between samples.

In Fig.4 it has been shown the autocorrelation function, log-log plot and changes of correlation dimension vs embedding dimension calculated for q = 0.0216 l/min, f = 10.62 Hz.

Obtained results allow us to estimate the proper value of time delay. In case under consideration is equal to 11 and embedding dimension proper for attractor reconstruction is equal to 2.

In Fig.5 it has been shown the part of time series for q = 0.0216 l/min, view of attractors and recurrence plots obtained for the beginning and end part of time series. Related locations of windows have been shown above the time series chart. The windows wide ware equal to 1000 samples, time delay 11 and embedding dimension 2. In Fig.5c when the values of time series is close to zero, in RP vertical and horizontal lines are visible. Decreasing of amplitude of time series causes the appearance of diagonal lines with smaller length (Fig.5d).

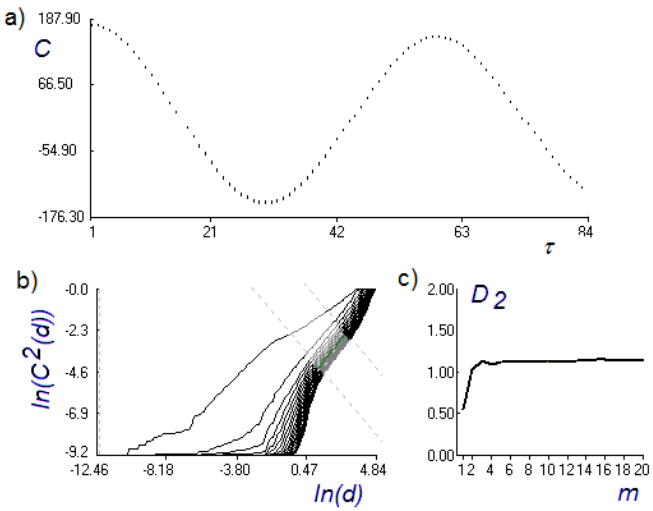

Figure 4 Example of analysis of entire time series. a) autocorrelation function, b) log-log plot, c) correlation dimension for q = 0.0216 l/min, f = 10.62 Hz

In Fig.6 it has been shown the changes of different quantities characterizing the RPs reconstructed for subsequent windows moving along the time series. The calculation has been made for window wide equal to 1000 samples, embedding dimension equal to 2, threshold ε equal to 1% of attractor diameter and time delay calculated separately for each time series.

Overall characteristic of moving RP

The changes of coefficient *RR* presented in Fig.6a show the overall characteristic of changes of subsequent recurrence plots for different time series. The decreasing of depth of water flooding to the nozzle in subsequent waiting times are visible as decreasing of the value of coefficient *RR*. Two such time periods were identified in the time series 1, 3 for time series 2. Similar behaviour of functions *RR*(*t*) are observed for another time series.

Characteristics of small changes of system state

Small changes of time series appear when maximum depth of water flooding nozzle is small. Such situations are indicated by vertical (horizontal) lines which appear in the RP (Fig.2c). Coefficients v_{max} and *TT* characterize the length of vertical (horizontal) lines in RP are shown in Fig.6b and c. Coefficient v_{max} indicates when the small changes of the system state appear. Function $v_{max}(t)$ consist of segments of constant line. The duration of time when the coefficient v_{max} has a constant value (Fig.6b) depends on the width of the window. The coefficient *TT* is a measure of average length of the vertical (horizontal) lines greater than 1. The Coefficient *TT* reaches maximum values for times series 1. It happens because the frequency of bubble departure is small. Also coefficient *TT* reaches high values for series 4 it is because in this case the situation when maximum depth of water flooding nozzle is small often occur.

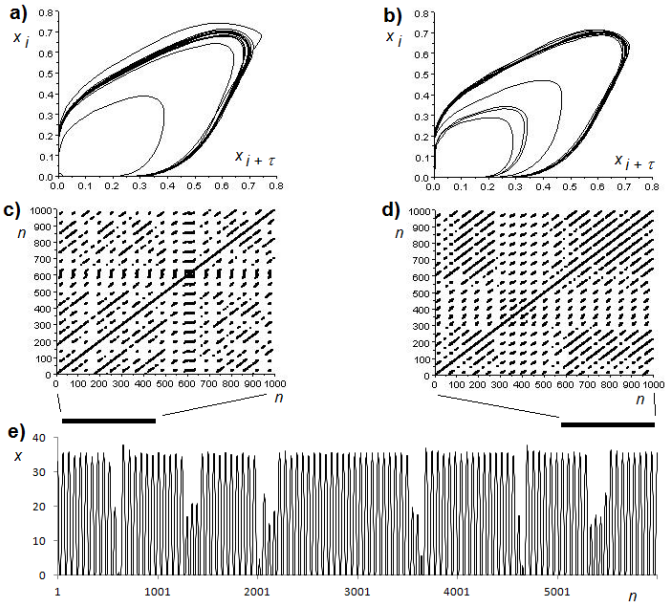

Figure 5 Part of time series for q = 0.0216 l/min, view of attractors and recurrence plots obtained for the beginning and end part of time series. a), b) 2D attractors, c), d) Recurrence plots. e) part of time series.

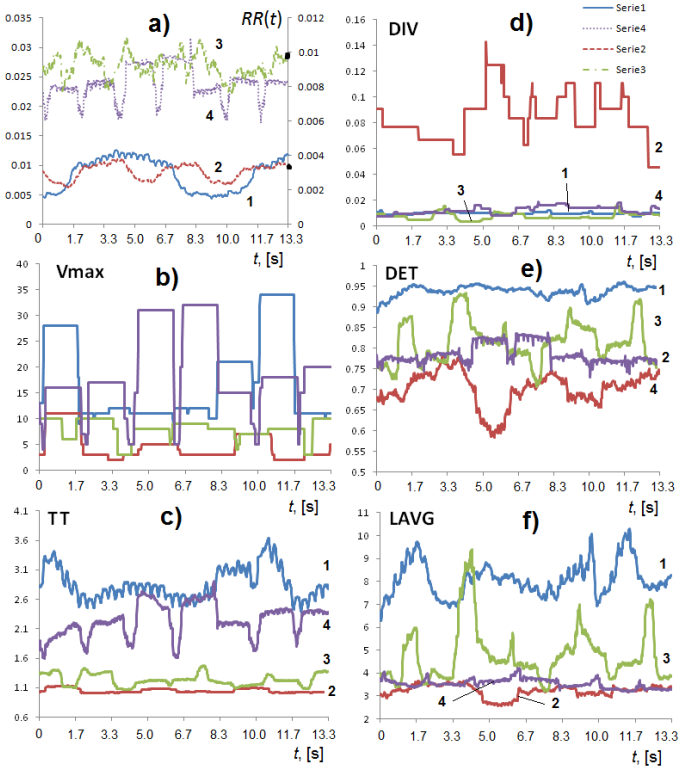

Figure 6 Results of calculations of quantities characterizing the moving RPs. Window width was equal to 1000 samples, embedding dimension equal to 2, threshold ε equal to 1% of attractor diameter and time delay calculated for each time series separately (35, 17, 11,7). a) Coefficients *RR*. b) Coefficients v_{max}. c) Coefficients *TT*. d) Coefficients *DIV*. e) Coefficients *DET*. f) Coefficients *LAVG*.

Characteristics of periodic or quasi periodic changes of system state

Periodic changes of system state appear when subsequent maximum depths of water flooding nozzle are similar. The length of diagonal lines is a measure of duration of oscillating character of the system. Increase of the average length of diagonal lines indicates that periodic processes are more present in the investigated system. In Fig.6 it has been shown the changes in time of three coefficients characterized by the diagonal lines in subsequent moving RP. In Fig.6d it has been shown the functions $DIV(t)$ which are calculated as $1/L_{max}$. The function *DIV* reaches the higher value for time series 2. In this case the subsequent values of large maximum depth of flooding water oscillate. Such changes causes that length of diagonal lines are small in comparison with other cases. In Fig.6e it has been shown the functions $DET(t)$. The value of the coefficient *DET* is the percentage of recurrence points which form diagonal lines greater than 1. Function $DET(t)$ reaches the maximum values for time series 1 and minimum value for time series 4. It means that in series 4 the duration of periodic changes of values of time series are longer than in series 1. Coefficient *LAVG* is the measure of average length of the diagonal lines, the function $LAVG(t)$ has been shown in Fig.6f. Obtained results correspond with results obtained for function $DET(t)$.

Chaotic dynamics of the system

Recurrence plot created for deterministic chaos system consists of segments of diagonal lines and isolated points. In cases under consideration the values of functions $DET(t)$ are greater than 50%. It means that more than half points of RPs form diagonal lines. From the other side the average length of diagonal lines (*LAVG*) is much lower than number of samples in the window (maximum length of diagonal lines is less than 300). Therefore, we can conclude that such behaviours of moving RPs are characteristic for deterministic chaos systems.

CONCLUSION

In the paper the time series describing the liquid-air interface positions in the glass nozzle have been analyzed. In recorded time series we can distinguish two kinds of changes of the position of liquid-air interface inside the nozzle. In the first kind, the changes have large amplitude and they seem to have periodic or quasi periodic character. In the other one, the amplitude of changes is lower than this one in previous case and the changes are not periodic. The increase of air liquid flow rate causes the decrease of duration of periodic changes. Despite the fact that obtained results of nonlinear analysis show that investigated time series have deterministic chaos character the periodic changes happen often for lower air volume flow rate. The chaotic bubble departures lead to bubble coalescences and finally to decreasing the area of liquid-gas interface. The understanding mechanisms of appearance of chaotic bubble departures can be useful in industrial applications where the area of liquid-gas interface plays an important role.

The analysis carried out in the paper show that for the low frequency of bubble departures (2.57±3.4% Hz) the liquid movement inside the glass nozzle loses its stability every time after about 7s period of time. This resulted in small variation (3.4%) of frequency of bubble departures. During the periodic liquid movement (in 7s period of time) the variations of frequency of bubble departures are about 0.1%. For the higher frequency of bubble departures its variation significantly increases from (10.67±14% Hz) up to 14%. In this case, time periods with periodic liquid movement disappear.

References

[1] Ruzicka, M.C., Bunganic, R. Drahos, J., 2009, Meniscus dynamics in bubble formation. Part I: *Experiment. Chem. Eng. Res. Des*., 87: 1349–1356.

[2] M.C. Ruzicka, R. Bunganic, J. Draho˘s, Meniscus dynamics in bubble formation. Part II: *Model, Chemical Engineering Research and Design*, 87 (2009), s. 1357–1365.

[3] Petr Stanovsky, Marek C. Ruzicka, Artur Martins, Jose A. Teixeira, Meniscus dynamics in bubble formation: A parametric study, *Chemical Engineering Science*, 66 (2011), s. 3258–3267.

[4] S.S. Dukhin, N.A. Mishchuk, V.B. Fainerman, R. Miller, Hydrodynamic processes in dynamic bubble pressure experiments 2. Slow meniscus oscillations, Colloids and Surfaces A: *Physicochemical and Engineering Aspects* 138 (1998) s. 51–63.

[5] S.S. Dukhin, V.I. Koval'chuk, V.B. Fainerman, R.Miller, Hydrodynamic processes in dynamic bubble pressure experiments Part 3. Oscillatory and aperiodic modes of pressure variation in the capillary, Colloids and Surfaces A: *Physicochemical and Engineering Aspects* 141 (1998), s 253–267.

[6] V.I. Koval'chuk, S.S. Dukhin, V.B. Fainerman, R. Miller, Hydrodynamic processes in dynamic bubble pressure experiments. 4. Calculation of magnitude and time of liquid penetration into capillaries, Colloids and Surfaces A: *Physicochemical and Engineering Aspects* 151 (1999), s 525–536.

[7] H.G Schuster., Deterministic Chaos. An Introduction, PWN, Warszawa 1993 (in Polish).

[8] E. Ott. Chaos in Dynamical Systems. WNT, 1997, in Polish.

[9] N. Marwan, M. C.Romano, M. Thiel, J. Kurths, Recurrence Plots for the Analysis of Complex Systems, *Physics Reports*, 2007, 438 (5-6), pp. 237-329. Recurrence Plots and Cross Recurrence Plots (www.recurrence-plot.tk).